INTERNATIONAL JOURNAL FOR NUMERICAL METHODS IN ENGINEERING, VOL. 37, 1039–1052 (1994)

INVESTIGATION OF REGULARIZATION PARAMETERS AND ERROR ESTIMATING IN INVERSE ELASTICITY PROBLEMS

ANTOINETTE M. MANIATTY

Department of Mechanical Engineering, Aeronautical Engineering and Mechanics, Rensselaer Polytechnic Institute, Troy, NY 12180, U.S.A.

NICHOLAS J. ZABARAS

Sibley School of Mechanical and Aerospace Engineering, Cornell University, Ithaca, NY 14853, U.S.A.

SUMMARY

The method of Tarantola[1] based on Bayesian statistical theory for solving general inverse problems is applied to inverse elasticity problems and is compared to the spatial regularization technique presented in Schnur and Zabaras.[2] It is shown that when normal Gaussian distributions are assumed and the error in the data is uncorrelated, the Bayesian statistical theory takes a form similar to the deterministic regularization method presented earlier in Schnur and Zabaras.[2] As such, the statistical theory can be used to provide a statistical interpretation of regularization and to estimate error in the solution of the inverse problem. Examples are presented to demonstrate the effect of the regularization parameters and the error in the initial data on the solution.

1. INTRODUCTION

Most problems analysed in solid mechanics are posed as direct problems, where the problem is to solve a governing system of equations (e.g. the balance of momentum equations, the constitutive equations and the kinematic equations) given sufficient boundary and initial conditions, i.e. tractions, displacements and initial stresses, for the resulting displacement, stress and strain fields. However, many practical problems do not fall into this category. In particular, there are many cases where the boundary conditions are not sufficiently known to give a unique solution, but some additional data, either in the form of overspecified boundary conditions on another part of the boundary or a part of the solution internal to the domain, is known approximately from measurements. This would be an inverse problem. Consider, for example, contact problems where it may be very difficult to measure the conditions in the contact region, but on the other hand, it may be easy to measure both tractions and displacements on another part of the boundary (overspecified boundary conditions) or displacements internal to the domain (part of the solution). Now the goal would be to use this additional information to solve for the unknown boundary conditions, and then to solve the direct problem as usual. There are also inverse problems where the parameters in the governing equations are unknown. This would be a parameter estimation problem and is not considered here.

There has been only limited research on inverse problems in solid mechanics with the emphasis on dynamic problems.[3–5] The work presented herein focuses on the linear elastic static problem with unspecified conditions on part of the boundary. This problem was previously studied by

CCC 0029–5981/94/061039–14$9.00

Received 30 November 1992
Revised 25 February 1993

Maniatty *et al.*,[6] who used simple diagonal regularization in conjunction with the finite element method to determine the unknown traction boundary conditions for a two-dimensional elastic problem. Spatial regularization was introduced in conjunction with the boundary element method by Zabaras *et al.*[7] and with the finite element method by Schnur and Zabaras.[2] Schnur and Zabaras[2] also presented the keynode method, a polynomial approximation technique. The spatial regularization method was adapted to accomodate two-dimensional elasto-viscoplastic material behaviour in Zabaras and Schnur.[8] Other static problems investigated include the estimation of elastic parameters in elastic bodies from displacement and/or traction data (see e.g. References 9 and 10). From residual surface displacements resulting from unknown loadings, Mura[11] evaluated plastic strains. Gao and Mura[12] evaluated residual stresses using the boundary integral method and later utilized this method to assess the interfacial damage between the matrix and an individual fibre in composite materials.[13]

2. DEFINITION OF THE PROBLEM

Consider a two-dimensional domain B with boundary ∂B. The problem definition is similar to that for the usual direct, isotropic, linear elasticity problem, except the boundary conditions are unknown on part of the boundary. Let displacements $\hat{u}_i$ be specified on part of the boundary ∂B_{1i} and tractions $\hat{t}_i$ be specified on part of the boundary ∂B_{2i} where $\partial B_{1i} \cap \partial B_{2i} = \emptyset$, but in this case there still remains another part of the boundary $\partial B_{3i} = \partial B_i - (\partial B_{1i} \cup \partial B_{2i})$, where the boundary conditions are unknown. Instead, additional displacements $\hat{u}_i^*$ are specified at discrete locations, $\mathbf{x}_\beta$, $\beta = 1, N_s$, either internal to the domain or on part of the boundary which already has tractions specified (i.e. overspecified boundary conditions). These additional displacements are known from measurements (N_s is the number of sensor locations) which have some degree of random error. Summarizing the problem in equation form gives

$$\operatorname{div} \mathbf{T} = \mathbf{0} \quad \text{on } B \tag{1}$$

$$\mathbf{E} = \tfrac{1}{2}[\nabla \mathbf{u} + (\nabla \mathbf{u})^{\mathrm{T}}] \tag{2}$$

$$\mathbf{T} = 2\mu \mathbf{E} + \lambda \operatorname{tr}(\mathbf{E})\, \mathbf{I} \tag{3}$$

$$\mathbf{e}_i \cdot \mathbf{u} = \hat{u}_i, \quad \text{on } \partial B_{1i} \tag{4}$$

$$\mathbf{e}_i \cdot (\mathbf{T}\mathbf{n}) = \hat{t}_i, \quad \text{on } \partial B_{2i} \tag{5}$$

$$\mathbf{e}_i \cdot \mathbf{u}(\mathbf{x}_\beta) \approx \hat{u}_i^*(\mathbf{x}_\beta), \quad \mathbf{x}_\beta \in (B \cup \partial B_{2i}), \quad \mathbf{x}_\beta \notin (\partial B_{1i} \cup \partial B_{3i}) \tag{6}$$

with $\beta = 1, N_s$, $i = 1, 2$, and where $\mathbf{T}$ is the stress tensor, $\mathbf{E}$ is the infinitesimal strain tensor, μ and λ are the Lamé parameters, $\mathbf{n}$ is the outward unit normal on ∂B, and $\mathbf{e}_i$ is an orthonormal set of basis vectors for the two-dimensional space. Equations (1)–(3) are the usual field equations for linear elasticity, equations (4) and (5) are the usual boundary conditions, and equation (6) gives the additional displacement information for the inverse problem. The goal now is to find the unknown tractions $\tilde{t}_i$ on the boundary ∂B_{3i}. Then the problem can be solved in the usual direct manner.

3. FINITE ELEMENT DISCRETIZATION

After discretization and applying the finite element method, a system of equations of the following form results

$$\{\mathbf{f}(\{\hat{\mathbf{t}}\})\} + \{\mathbf{f}(\{\tilde{\mathbf{t}}\})\} = [\mathbf{K}]\{\mathbf{u}\} \tag{7}$$

where $\{\mathbf{f}(\{\hat{\mathbf{t}}\})\}$ and $\{\mathbf{f}(\{\tilde{\mathbf{t}}\})\}$ are the parts of the force vector due to the known and unknown tractions, respectively, and where $[\mathbf{K}]$ and $\{\mathbf{u}\}$ are the usual linear elastic stiffness matrix and the vector of nodal displacements, respectively. Writing a Taylor expansion for $\{\mathbf{f}(\{\tilde{\mathbf{t}}\})\}$ around $\{\tilde{\mathbf{t}}\} = \{\mathbf{0}\}$ with given $\{\hat{\mathbf{t}}\}$ and equating it to equation (7) gives

$$\{\mathbf{f}(\{\tilde{\mathbf{t}}\})\} = [\mathbf{K}]\left[\frac{\partial \mathbf{u}}{\partial \tilde{\mathbf{t}}}\right]\{\tilde{\mathbf{t}}\} = [\mathbf{K}]\{\mathbf{u}\} - \{\mathbf{f}(\{\hat{\mathbf{t}}\})\}$$

or

$$\left[\frac{\partial \mathbf{u}}{\partial \tilde{\mathbf{t}}}\right]\{\tilde{\mathbf{t}}\} = \{\mathbf{u}\} - \{\bar{\mathbf{u}}\} \tag{8}$$

where

$$\{\bar{\mathbf{u}}\} = [\mathbf{K}]^{1}\{\mathbf{f}(\{\hat{\mathbf{t}}\})\}$$

Comparing with equation (7), it can be seen that $\{\bar{\mathbf{u}}\}$ represents the vector of displacements due only to the known tractions on ∂B_{2i} with zero tractions on ∂B_{3i}. It should be noted that equation (8) is exact because this is a linear problem. Since only part of $\{\mathbf{u}\}$ is known, i.e. $\{\mathbf{u}^*\} = [\mathbf{Q}]\{\mathbf{u}\}$ where $\{\mathbf{u}^*\}$ is the vector of modelled displacements corresponding to the measured displacements $\{\hat{\mathbf{u}}^*\}$, equation (8) must be rewritten as

$$[\mathbf{S}^*]\{\tilde{\mathbf{t}}\} = \{\mathbf{u}^*\} - [\mathbf{Q}]\{\bar{\mathbf{u}}\} \tag{9}$$

where

$$[\mathbf{S}^*] = [\mathbf{Q}]\left[\frac{\partial \mathbf{u}}{\partial \tilde{\mathbf{t}}}\right]$$

is the sensitivity matrix. The matrix $[\mathbf{Q}]$ is defined by the sensor locations, which coincide here with nodal points in the finite element mesh. Note that $[\partial \mathbf{u}/\partial \tilde{\mathbf{t}}]$ can be calculated explicitly from

$$\left[\frac{\partial \mathbf{u}}{\partial \tilde{\mathbf{t}}}\right] = [\mathbf{K}]\left[\frac{\partial \mathbf{f}}{\partial \tilde{\mathbf{t}}}\right]$$

where $[\partial \mathbf{f}/\partial \tilde{\mathbf{t}}]$ can be determined independently of $\{\tilde{\mathbf{t}}\}$ since $\{\mathbf{f}(\{\tilde{\mathbf{t}}\})\}$ is linear in $\{\tilde{\mathbf{t}}\}$. Now the goal is to minimize the following error measure:

$$E = \tfrac{1}{2}(\{\hat{\mathbf{u}}^*\} - \{\mathbf{u}^*\})^{\mathrm{T}}(\{\hat{\mathbf{u}}^*\} - \{\mathbf{u}^*\})$$

with respect to $\{\tilde{\mathbf{t}}\}$. In general, the solution to the above minimization problem for $\{\tilde{\mathbf{t}}\}$ is unstable and may not be unique.

4. SOLUTION BY SPATIAL REGULARIZATION

In order to obtain a stable solution, one method Schnur and Zabaras[2] incorporated was spatial regularization. In this method, the following minimization is solved for $\{\tilde{\mathbf{t}}\}$:

$$\min_{\{\tilde{\mathbf{t}}\}} [(\{\hat{\mathbf{u}}^*\} - \{\mathbf{u}^*\})^{\mathrm{T}}(\{\hat{\mathbf{u}}^*\} - \{\mathbf{u}^*\}) + \Omega] \tag{10}$$

where Ω is the following smoothing function

$$\Omega = \sum_{i=1}^{2}\left[\alpha_0^i \int_{\partial B_{3i}} (\tilde{t}_i)^2\,\mathrm{d}s + \alpha_1^i \int_{\partial B_{3i}} \left(\frac{\partial \tilde{t}_i}{\partial s}\right)^2 \mathrm{d}s + \alpha_2^i \int_{\partial B_{3i}} \left(\frac{\partial^2 \tilde{t}_i}{\partial s^2}\right)^2 \mathrm{d}s\right] \tag{11}$$

and where $\alpha_j^i > 0$, $i = 1, 2$, $j = 0, 2$. The parameters α_0^i, α_1^i and α_2^i are the zeroth; first, and second-order regularization parameters, respectively, for the ith degree of freedom. Using finite element interpolations for $\tilde{t}_i$ in equation (11) gives

$$\Omega = \{\tilde{\mathbf{t}}\}^{\mathrm{T}}[\mathbf{F}]\{\tilde{\mathbf{t}}\}$$

where [F] is the spatial regularization matrix. Substituting this and equation (9) into equation (10) and minimizing results in the following system:

$$([\mathbf{S}^*]^{\mathrm{T}}[\mathbf{S}^*] + [\mathbf{F}])\{\tilde{\mathbf{t}}\} = [\mathbf{S}^*]^{\mathrm{T}}(\{\hat{\mathbf{u}}^*\} - [\mathbf{Q}]\{\bar{\mathbf{u}}\}) \tag{12}$$

Equation (12) can then be solved for $\{\tilde{\mathbf{t}}\}$. Schnur and Zabaras[2] used this method successfully to solve a variety of inverse elasticity problems of this form. The questions which remain unanswered are how do we choose the regularization parameters and does it matter. Tikhonov and Arsenin[14] and Beck *et al.*[15] suggest guidelines for selecting the regularization parameters in inverse problems, and Artyukhin[16] advocates the so-called residual method for finding the regularization parameters. However, a consensus has not yet been reached on a general method for obtaining the regularization parameter. In the following section, a statistical approach is used to obtain a solution to the inverse problem which also provides a means to estimate the error. The form of the solution obtained by the statistical method is similar to that obtained by the regularization method and is compared to the regularization method in order to investigate the significance of the regularization parameters.

5. SOLUTION BY STATISTICAL APPROACH

A general statistical approach to solving inverse problems based on Bayesian theory is applied in this section. Let

$$\{\mathbf{u}'_0\} = \{\hat{\mathbf{u}}^*\} - [\mathbf{Q}]\{\bar{\mathbf{u}}\}$$

represent the observed data, i.e. the measured displacements minus the part of the displacements at the sensor locations due to the known tractions. Furthermore, let $\{\mathbf{u}'\}$ be the true displacement vector corresponding to the observed displacement vector $\{\mathbf{u}'_0\}$ According to the Bayesian theory, the *a priori* states of information regarding $\{\mathbf{u}'\}$ and $\{\tilde{\mathbf{t}}\}$ can be expressed as probability density functions. For example, if the statistics regarding the accuracy of the measured displacements $\{\hat{\mathbf{u}}^*\}$ and the specified tractions $\{\hat{\mathbf{t}}\}$ are known (e.g. standard deviations, etc.) then a probability density function can be constructed for $\{\mathbf{u}'\}$. The *a priori* information on the unknown tractions $\{\tilde{\mathbf{t}}\}$, in this case regarding the smoothness of the tractions, can also generally be expressed in terms of a probability density function. Furthermore, since a finite element model, which is an approximation of the physical problem, is used, a probability density function can be used to describe this uncertainty as well. Let $\xi(\{\mathbf{u}'\}, \{\tilde{\mathbf{t}}\})$ be the joint probability density function representing the *a priori* information on both the data $\{\mathbf{u}'\}$ and the model parameters $\{\tilde{\mathbf{t}}\}$, and let $\Theta(\{\mathbf{u}'\}|\{\tilde{\mathbf{t}}\})$ be the conditional probability density function representing the physical correlation between $\{\mathbf{u}'\}$ and $\{\tilde{\mathbf{t}}\}$. These states of information can be combined following the method of Tarantola[1] to give the *a posteriori* information on $\{\mathbf{u}'\}$ and $\{\tilde{\mathbf{t}}\}$ in the form of the following joint probability density function:

$$p(\{\mathbf{u}'\}, \{\tilde{\mathbf{t}}\}) = \frac{\xi(\{\mathbf{u}'\}, \{\tilde{\mathbf{t}}\})\Theta(\{\mathbf{u}'\}|\{\tilde{\mathbf{t}}\})\mu_{\tilde{t}}(\{\tilde{\mathbf{t}}\})}{\mu(\{\mathbf{u}'\}, \{\tilde{\mathbf{t}}\})} \tag{13}$$

where $\mu(\{\mathbf{u}'\}, \{\tilde{\mathbf{t}}\})$ represents the state of null information for $\{\mathbf{u}'\}$ and $\{\tilde{\mathbf{t}}\}$ which effectively acts as a scaling parameter so that the area under the *a posteriori* probability density function $p(\{\mathbf{u}'\}, \{\tilde{\mathbf{t}}\})$

is equal to one. The function $\mu_{\tilde{t}}(\{\tilde{\mathbf{t}}\})$ is the marginal non-informative probability density function for $\{\tilde{\mathbf{t}}\}$ representing the state of null information for $\{\tilde{\mathbf{t}}\}$, which in this equation acts to scale the conditional probability density function $\Theta(\{\mathbf{u}'\}|\{\tilde{\mathbf{t}}\})$. Since in this case, the data $\{\mathbf{u}'\}$ is independent of the *a priori* information on $\{\tilde{\mathbf{t}}\}$, $\xi(\{\mathbf{u}'\}\{\tilde{\mathbf{t}}\}) = \xi_{u'}(\{\mathbf{u}'\})\xi_{\tilde{t}}(\{\tilde{\mathbf{t}}\})$ and $\mu(\{\mathbf{u}'\}, \{\tilde{\mathbf{t}}\}) = \mu_{u'}(\{\mathbf{u}'\})\mu_{\tilde{t}}(\{\tilde{\mathbf{t}}\})$, where $\xi_{u'}$, $\xi_{\tilde{t}}$, $\mu_{u'}$ and $\mu_{\tilde{t}}$ are marginal probability density functions.

The *a posteriori* information on the unknown tractions is the general solution to the inverse problem. This is given by the marginal probability density function $p_{\tilde{t}}(\{\tilde{\mathbf{t}}\})$, which is defined as

$$p_{\tilde{t}}(\{\tilde{\mathbf{t}}\}) = \int_D p(\{\mathbf{u}'\}, \{\tilde{\mathbf{t}}\})\,\mathrm{d}\{\mathbf{u}'\} = \xi_{\tilde{t}}(\{\tilde{\mathbf{t}}\})\int_D \frac{\xi_{u'}(\{\mathbf{u}'\})\,\Theta(\{\mathbf{u}'\}|\{\tilde{\mathbf{t}}\})}{\mu_{u'}(\{\mathbf{u}'\})}\mathrm{d}\{\mathbf{u}'\} \tag{14}$$

where D is the data space on which $\{\mathbf{u}'\}$ is defined. Now the problem is to define the probability density functions in equation (14) and then evaluate $p_{\tilde{t}}(\{\tilde{\mathbf{t}}\})$. From the probability density function $p_{\tilde{t}}(\{\tilde{\mathbf{t}}\})$, it is possible to determine the expected values of the components of $\{\tilde{\mathbf{t}}\}$ and error bars for the components based on standard deviations.

If the errors in the data and the model are assumed to be Gaussian, then $\xi_{u'}(\{\mathbf{u}'\})$ and $\Theta(\{\mathbf{u}'\}|\{\tilde{\mathbf{t}}\})$ can be expressed in the following form:

$$\frac{\xi_{u'}(\{\mathbf{u}'\})}{\mu_{u'}(\{\mathbf{u}'\})} = ((2\pi)^{2N_s}\det[\mathbf{C}_{u'}])^{1/2}\exp[-\tfrac{1}{2}(\{\mathbf{u}'\} - \{\mathbf{u}'_0\})^{\mathrm{T}}[\mathbf{C}_{u'}]^{-1}(\{\mathbf{u}'\} - \{\mathbf{u}'_0\})] \tag{15}$$

$$\Theta(\{\mathbf{u}'\}|\{\tilde{\mathbf{t}}\}) = ((2\pi)^{2N_s}\det[\mathbf{C}_T])^{1/2}\exp[-\tfrac{1}{2}(\{\mathbf{u}'\} - [\mathbf{S}^*]\{\tilde{\mathbf{t}}\})^{\mathrm{T}}[\mathbf{C}_T]^{-1}(\{\mathbf{u}'\} - [\mathbf{S}^*]\{\tilde{\mathbf{t}}\})] \tag{16}$$

where $[\mathbf{C}_{u'}]$ and $[\mathbf{C}_T]$ are the covariance operators expressing the uncertainty in the data and the model, respectively. Substituting equations (15) and (16) into the integral in equation (14) and performing the integration gives

$$\int_D \frac{\xi_{u'}(\{\mathbf{u}'\})\,\Theta(\{\mathbf{u}'\}|\{\tilde{\mathbf{t}}\})}{\mu_{u'}(\{\mathbf{u}'\})}\mathrm{d}\{\mathbf{u}'\} = K\exp[-\tfrac{1}{2}(\{\mathbf{u}'_0\} - [\mathbf{S}^*]\{\tilde{\mathbf{t}}\})^{\mathrm{T}} \\ ([\mathbf{C}_{u'}] + [\mathbf{C}_T])^{-1}(\{\mathbf{u}'_0\} - [\mathbf{S}^*]\{\tilde{\mathbf{t}}\})] \tag{17}$$

where K is a constant. The proof of this result is given by Tarantola.[1] From equation (17), it can be seen that the Gaussian assumption has the useful result that the observational errors and the modelization errors simply combine by addition of the respective covariance operators, i.e.

$$[\mathbf{C}_D] = [\mathbf{C}_{u'}] + [\mathbf{C}_T]$$

where $[\mathbf{C}_D]$ is the combined covariance operator expressing the uncertainties in the model and the data.

Now if the *a priori* information on the solution has a Gaussian form also, then

$$\xi_{\tilde{t}}(\{\tilde{\mathbf{t}}\}) = ((2\pi)^{2N_t}\det[\mathbf{C}_\Omega])^{1/2}\exp[-\tfrac{1}{2}(\{\tilde{\mathbf{t}}\} - \{\tilde{\mathbf{t}}_0\})^{\mathrm{T}}[\mathbf{C}_\Omega]^{-1}(\{\tilde{\mathbf{t}}\} - \{\tilde{\mathbf{t}}_0\})] \tag{18}$$

where $[\mathbf{C}_\Omega]$ is the covariance operator expressing the uncertainty in the *a priori* information, $\{\tilde{\mathbf{t}}_0\}$ is an initial guess for $\{\tilde{\mathbf{t}}\}$, and N_t is the number of discrete unknown tractions. Substituting (17) and (18) into (14) gives

$$p_{\tilde{t}}(\{\tilde{\mathbf{t}}\}) = C\exp[-m(\{\tilde{\mathbf{t}}\})]$$

$$m(\{\tilde{\mathbf{t}}\}) = \tfrac{1}{2}[([\mathbf{S}^*]\{\tilde{\mathbf{t}}\} - \{\mathbf{u}'_0\})^{\mathrm{T}}[\mathbf{C}_D]^{-1}([\mathbf{S}^*]\{\tilde{\mathbf{t}}\} - \{\mathbf{u}'_0\}) \\ + (\{\tilde{\mathbf{t}}\} - \{\tilde{\mathbf{t}}_0\})^{\mathrm{T}}[\mathbf{C}_\Omega]^{-1}(\{\tilde{\mathbf{t}}\} - \{\tilde{\mathbf{t}}_0\})] \tag{19}$$

where C is a constant.

The expected solution for $\{\tilde{\mathbf{t}}\}$ (maximum likelihood point) is that which maximizes $p_{\tilde{t}}(\{\tilde{\mathbf{t}}\})$ and therefore, minimizes $m(\{\tilde{\mathbf{t}}\})$. Performing the minimization gives

$$\langle\{\tilde{\mathbf{t}}\}\rangle = ([\mathbf{S}^*]^{\mathrm{T}}[\mathbf{C}_D]^{-1}[\mathbf{S}^*] + [\mathbf{C}_\Omega]^{-1})^{-1}([\mathbf{S}^*]^{\mathrm{T}}[\mathbf{C}_D]^{-1}\{\mathbf{u}'_0\} + [\mathbf{C}_\Omega]^{-1}\{\tilde{\mathbf{t}}_0\}) \tag{20}$$

where $\langle\cdot\rangle$ indicates the expected value. The corresponding covariance operator which will be used to obtain the standard deviations can be determined by expressing equation (19) in normal form. First, rearranging the terms in $m(\{\tilde{\mathbf{t}}\})$ and substituting in $\langle\{\tilde{\mathbf{t}}\}\rangle$ from equation (20) gives

$$\begin{aligned} m(\{\tilde{\mathbf{t}}\}) = \tfrac{1}{2}[(\{\tilde{\mathbf{t}}\} - \langle\{\tilde{\mathbf{t}}\}\rangle)^{\mathrm{T}}[\mathbf{C}_{\tilde{t}}]^{-1}(\{\tilde{\mathbf{t}}\} - \langle\{\tilde{\mathbf{t}}\}\rangle) - \langle\{\tilde{\mathbf{t}}\}\rangle^{\mathrm{T}}[\mathbf{C}_{\tilde{t}}]^{-1}\langle\{\tilde{\mathbf{t}}\}\rangle \\ + \{\mathbf{u}'_0\}^{\mathrm{T}}[\mathbf{C}_D]^{-1}\{\mathbf{u}'_0\} + \{\tilde{\mathbf{t}}_0\}^{\mathrm{T}}[\mathbf{C}_\Omega]^{-1}\{\tilde{\mathbf{t}}_0\}] \end{aligned} \tag{21}$$

where

$$[\mathbf{C}_{\tilde{t}}] = ([\mathbf{S}^*]^{\mathrm{T}}[\mathbf{C}_D]^{-1}[\mathbf{S}^*] + [\mathbf{C}_\Omega]^{-1})^{-1} \tag{22}$$

Now substituting this into equation (19) for $p_{\tilde{t}}(\{\tilde{\mathbf{t}}\})$ and observing that the last three terms in the above equations are constant gives the normal form of equation (19)

$$p_{\tilde{t}}(\{\tilde{\mathbf{t}}\}) = C' \exp[-\tfrac{1}{2}(\{\tilde{\mathbf{t}}\} - \langle\{\tilde{\mathbf{t}}\}\rangle)^{\mathrm{T}}[\mathbf{C}_{\tilde{t}}]^{-1}(\{\tilde{\mathbf{t}}\} - \langle\{\tilde{\mathbf{t}}\}\rangle)] \tag{23}$$

where the last three terms have been absorbed into the constant C'. Therefore, $[\mathbf{C}_{\tilde{t}}]$ defined in equation (22) is the covariance operator for this distribution.

To compare this result with that given in Section 4 using spatial regularization, consider if the correlations in the modelization errors are neglected, and it is assumed that the error in the data is uncorrelated. Then $[\mathbf{C}_D]$ reduces to a diagonal matrix. Furthermore, if the variance σ_D^2 is assumed to be the same for each corresponding datapoint, $[\mathbf{C}_D]$ becomes simply

$$[\mathbf{C}_D] = \sigma_D^2[\mathbf{I}]$$

and then equations (20) and (22) reduce to

$$\langle\{\tilde{\mathbf{t}}\}\rangle = ([\mathbf{S}^*]^{\mathrm{T}}[\mathbf{S}^*] + \sigma_D^2[\mathbf{C}_\Omega]^{-1})^{-1}([\mathbf{S}^*]^{\mathrm{T}}\{\mathbf{u}'_0\} + \sigma_D^2[\mathbf{C}_\Omega]^{-1}\{\tilde{\mathbf{t}}_0\}) \tag{24}$$

$$[\mathbf{C}_{\tilde{t}}] = \sigma_D^2([\mathbf{S}^*]^{\mathrm{T}}[\mathbf{S}^*] + \sigma_D^2[\mathbf{C}_\Omega]^{-1})^{-1} \tag{25}$$

Comparing equation (24) with equation (12), if the initial guess for $\{\tilde{\mathbf{t}}\}$ is $\{\tilde{\mathbf{t}}_0\} = \{\mathbf{0}\}$, then the regularization matrix $[\mathbf{F}]$ corresponds to $\sigma_D^2[\mathbf{C}_\Omega]^{-1}$. Equating $[\mathbf{F}]$ and $\sigma_D^2[\mathbf{C}_\Omega]^{-1}$ and expanding $[\mathbf{F}]$ gives

$$[\mathbf{F}] = \sum_{i=1}^{2}(\alpha_0^i[\mathbf{R}_0]^i + \alpha_1^i[R_1]^i + \alpha_2^i[\mathbf{R}_2]^i) = \sigma_D^2[\mathbf{C}_\Omega]^{-1} \tag{26}$$

Therefore, α_j^i represents the degree of uncertainty in the displacement data and the model, represented by σ_D^2, with respect to the degree of uncertainty in the jth order smoothness of the solution. So as the uncertainty in the displacement data and the model increases, the values of α_j^i should also increase, while as the uncertainty in the jth order smoothness increases, the values of α_j^i should decrease. It should be noted that taking $\{\tilde{\mathbf{t}}_0\} = \{\mathbf{0}\}$ is reasonable if there is no *a priori* estimate of $\{\tilde{\mathbf{t}}\}$ since it satisfies the *a priori* smoothness assumption on $\{\tilde{\mathbf{t}}\}$ which may be all that is known regarding $\{\tilde{\mathbf{t}}\}$.

Furthermore, an estimate of the error in the solution can be obtained by calculating the covariance $[\mathbf{C}_{\tilde{t}}]$ from

$$[\mathbf{C}_{\tilde{t}}] = \sigma_D^2([\mathbf{S}^*]^{\mathrm{T}}[\mathbf{S}^*] + [\mathbf{F}])^{-1} \tag{27}$$

since the diagonal elements of $[\mathbf{C}_{\tilde{t}}]$ will be the variances $\{\sigma_{\tilde{t}}^2\}$ for $\{\tilde{\mathbf{t}}\}$. This equation shows that as the uncertainty in the displacement data, the model and the smoothness increase, the uncertainty in the solution represented by $\{\sigma_{\tilde{t}}^2\}$ will also increase.

As a final point, something must be said about the effect of assuming normal Gaussian density functions and uncorrelated errors in the model and the data. The only two characteristics of interest here regarding the density function of $\{\tilde{\mathbf{t}}\}$ are the position of the 'centre' and the 'error bounds'. The position of the 'centre' (maximum likelihood point) will not be affected as long as the actual density functions are symmetric. Furthermore, the behaviour of the density functions far from the centre is only crucial if stray points far from the centre exist. If the error bounds on the data and model are known precisely, i.e. it is known that no points can occur outside these bounds, then the assumption of a normal distribution will apply well. It is usually reasonable to assume that the errors in the measured displacements are uncorrelated, but this is not the case for modelization errors. However, assuming that the errors are uncorrelated is known to give a conservative estimate if the errors are actually correlated since neglecting the correlations represents a lower state of information.

6. CHOOSING THE REGULARIZATION PARAMETERS

It is difficult to quantify *a priori* the degree of confidence one should have in the smoothness of the solution. Therefore, it is usually necessary to solve the problem with several different sets of regularization parameters α_j^i in order to determine which set gives the best solution, i.e. the stable solution with the smallest error bars. Intuitively, it is expected that the elements of $[\mathbf{F}]$ should be small relative to the elements of $[\mathbf{S}^*]^T[\mathbf{S}^*]$ because minimizing the difference between the model displacements $\{\mathbf{u}^*\}$ and the measured displacements $\{\hat{\mathbf{u}}^*\}$ in equation (10) is of primary importance, while minimizing the smoothing function Ω is required only to stabilize the solution. The effect of the regularization parameters on the solution beyond enforcing stability should be kept to a minimum. This is the methodology followed by Schnur and Zabaras.[2] At the same time, it is desired to find the maximum values of α_j^i allowable because this minimizes the elements of $[\mathbf{C}_{\tilde{t}}]$ which will give the smallest error bars. Therefore, the first guess of α_j^i should be small with the elements of $[\mathbf{F}]$ being four or five orders of magnitude less than the elements of $[\mathbf{S}^*]^T[\mathbf{S}^*]$. This is generally enough to stabilize the solution, but will result in very large error bars. Then the values of the parameters α_j^i should be gradually increased until the solution starts to vary with the regularization parameters. When this happens, the regularization parameters are too large and are beginning to dominate the solution. Therefore, the solution with the largest regularization parameters that do not yet dominate the solution should be taken as the final solution. Domination of the regularization parameters on the solution is equivalent to expressing overconfidence in the smoothness of the solution.

The solution should be (relatively) invariant to the choice of regularization parameters α_j^i over one or more orders of magnitude. If the solution is found to depend always on the choice of regularization parameters, then the assumption of smoothness is either incorrect or insufficient and, therefore, a stable solution with any degree of confidence cannot be obtained. If this is the case, more information is needed to solve the problem.

7. NUMERICAL EXAMPLES

Two examples are presented to demonstrate the algorithm and error estimating capabilities. The first example involves a square plate assumed to be loaded in a state of plane stress as shown in Figure 1. Thirty-six eight-node isoparametric elements were used to model the plate. The length

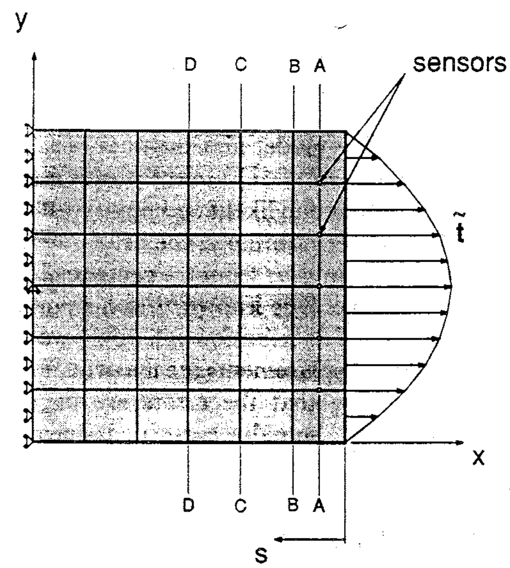

Figure 1. Geometry and loading condition for example 1

of each side of the plate is $L = 6$ m, the modulus of elasticity is taken as $E = 30$ GPa and Poisson's ratio as $\nu = 0{\cdot}30$. The plate is fixed in the x direction along the boundary $x = 0$ and one point is fixed in the y direction to constrain rigid body motion. The prescribed normal traction condition on the right-hand side of the plate is $t_x(y) = -\frac{1}{9}y^2 + \frac{2}{3}y$ (MPa). The direct problem is first solved and then the data from the solution with random error superimposed is used to predict inversely the traction condition on the right-hand side of the plate. The displacements at five 'sensor' locations along line AA (denoted in Figure 1 with circles) were used to predict the tractions at eleven nodes on the boundary (the zero tractions for the top and bottom nodes were assumed known). The displacements at the 'sensors' in the x-direction, u_x, were of the order of $O(u_x) = 0{\cdot}1$ mm and in the y direction, u_y, were of the order of $O(u_y) = 0{\cdot}001$ mm. Uniform random error represented by parameters ω_i, where $-\varepsilon \leqslant \omega_i \leqslant \varepsilon$, with $\varepsilon = 0{\cdot}002$ mm and $i = 1, 2N_s$, or ± 2 per cent of $O(u_x)$, was added to the displacement data to simulate measurement errors. Since a finite element model is used to get the displacement data and a finite element model is used in the inverse procedure with the same interpolation functions, the model is taken to be exact in this case, so modelization errors are not being considered.

Figure 2 illustrates the effect of different regularization parameters on the solution. In each case, the largest order of magnitude of the regularization parameter that did not start to affect the solution significantly was used. The regularization parameters given in the figure are in units of mm and MPa. First- and second-order regularization give approximately the same result, while zeroth order regularization gives a much poorer solution. This is because first- and second-order regularization apply stronger smoothness conditions on the solution which are necessary, since the solution is not unique and are appropriate in this case since the true solution is in fact smooth. Lamm[17] shows mathematically that as the order of regularization increases, so does the accuracy of the solution as long as the true solution exhibits that smoothness, which is what this result demonstrates. Figure 3 illustrates the effect of the order of magnitude of the regularization parameters on the solution for first-order regularization with $\alpha_0^1 = \alpha_0^2 = \alpha_2^1 = \alpha_2^2 = 0$, using the

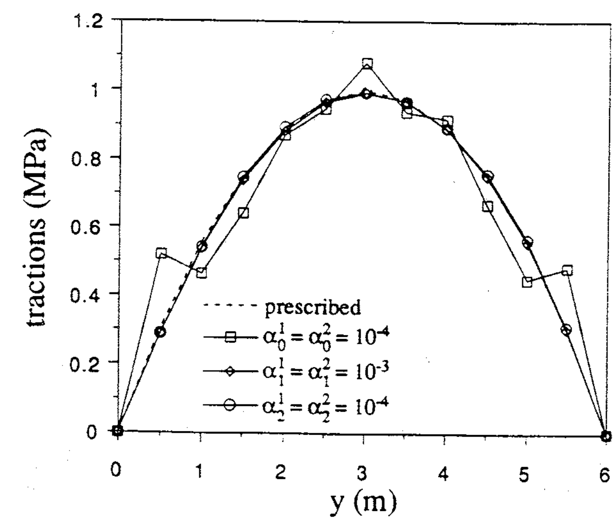

Figure 2. Effect of the order of regularization on the solution for example 1

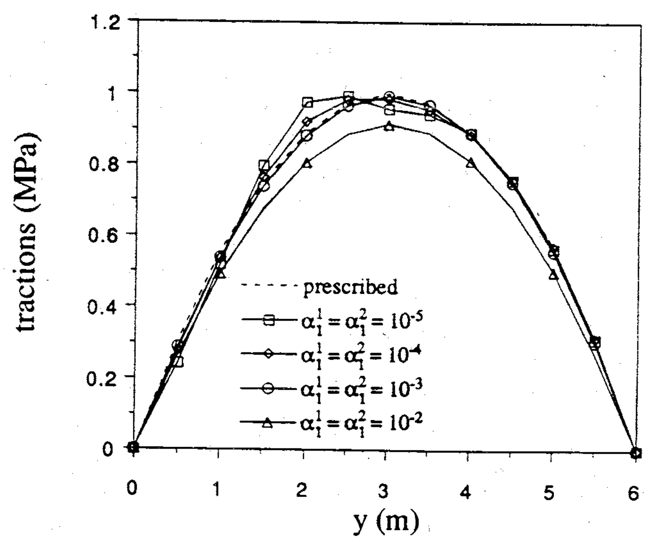

Figure 3. Effect of the order of magnitude of the regularization parameter for first-order regularization ($\alpha_0^1 = \alpha_0^2 = \alpha_2^1 = \alpha_2^2 = 0$) in connection with the solution of example 1

same random error input in each case as used in the previous example. For $\alpha_1^1 = \alpha_1^2 = 10^{-5}$ $(\text{mm/MPa})^2$, the solution is still slightly unstable, for $\alpha_1^1 = \alpha_1^2 = 10^{-4}$ $(\text{mm/MPa})^2$ and $\alpha_1^1 = \alpha_1^2 = 10^{-3}$ $(\text{mm/MPa})^2$, the solution varies very little, and then at $\alpha_1^1 = \alpha_1^2 = 10^{-2}$ $(\text{mm/MPa})^2$, the regularization parameter starts to dominate and have a significant effect.

Figure 4 shows the effect of the error in the displacement data on the error in the traction solution (represented by the standard deviation $\sigma_{\bar{t}}$) for the traction at the centre of the distribution (at $y = 3m$) where the prescribed traction takes on the value $t_x = 1$ MPa. Since a uniform

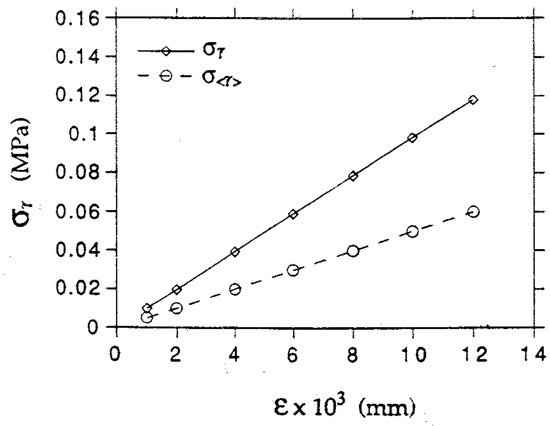

Figure 4. Effect of the error in the displacement data on the error in the traction at the centre of the distribution for example 1 using first-order regularization ($\alpha_1^1 = \alpha_1^2 = 10^{-3}$ (mm/MPa)^2)

distribution in the data was assumed, the standard deviation in the displacement data is $\sigma_{u'} = 0{\cdot}577\varepsilon$, where ε is the maximum deviation from the centre of the distribution as defined before. Only first-order regularization is used with $\alpha_1^1 = \alpha_1^2 = 10^{-3}$ (mm/MPa)^2. A Monte Carlo simulation was also performed with 50 trials at each datapoint for comparison. The standard deviation $\sigma_{<\tilde{t}>}$ in the predicted solution $\langle\{\tilde{\mathbf{t}}\}\rangle$ computed in the Monte Carlo simulation is plotted along with the predicted standard deviation. The predicted standard deviation is very conservative, especially at higher errors in the input. This may be due to the fact that the error in the data followed a uniform distribution rather than a Gaussian distribution as assumed in the analysis. At low errors in the input, additional errors due to truncation errors in the data start to become important and would need to be included to give a proper prediction of the error in the results. The displacement data used herein is truncated to five significant figures.

To illustrate the effect of sensor location, the problem was solved with five 'sensors' along lines AA, BB, CC and DD, each time with uniform random error with $\varepsilon = 0{\cdot}002$ mm, added to the displacements. The error in the traction at the centre of the distribution is plotted for the different sensor locations. Only first-order regularization was used. The regularization parameters for the case with the sensors along line AA were taken as $\alpha_1^1 = \alpha_1^2 = 10^{-3}$ (mm/MPa)^2. Since the sensitivity coefficients in [S*] become smaller as the sensors are placed further from the boundary, the regularization parameters must also be reduced so as not to dominate the solution. Therefore, the ratio α_1^i/s^*, $i = 1, 2$, was held constant for each case, where

$$s^* = \frac{\sum_{i=1}^{2N_t} \sum_{j=1}^{2N_t} S_{ij}^* S_{ij}^*}{2N_t}$$

is the average magnitude of the diagonal elements in $[\mathrm{S}^*]^{\mathrm{T}}[\mathrm{S}^*]$. For the first case along AA, $s^* = 0{\cdot}04521$ resulting in $\alpha_1^i/s^* = 0{\cdot}0221$. The values of α_1^i are then scaled for the remaining cases (sensors along BB, CC and DD) to maintain this ratio. The average predicted standard deviation and the actual calculated average deviation in the traction solutions are plotted in Figure 5, and it can be seen that the predicted standard deviation is quite conservative.

To examine the true statistics of the solution, a Monte-Carlo simulation was performed with 200 trials for the cash with $\varepsilon = 0{\cdot}002$ mm. The range of values computed for the traction at the

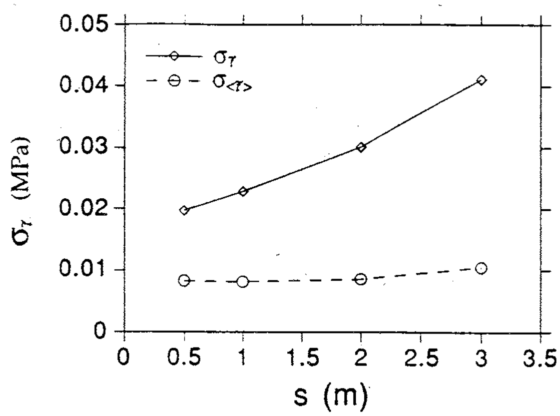

Figure 5. Effect of the sensor location on the error in the traction at the centre of the distribution for example 1 using only first-order regularization

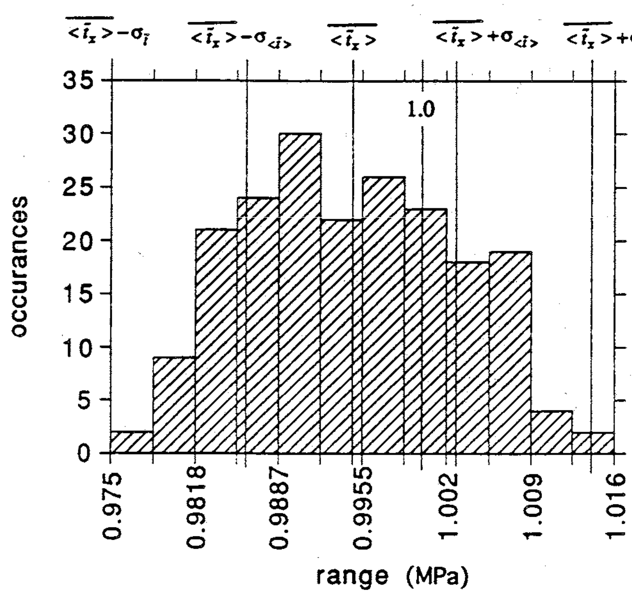

Figure 6. Histogram showing distribution of predicted tractions for 200 trials with $\varepsilon = 0{\cdot}002$ mm along with the true solution ($\tilde{t} = 1{\cdot}0$ MPa) and computed and predicted standard deviations $\sigma_{<\tilde{t}>}$ and $\sigma_{\tilde{t}}$.

centre of the distribution denoted $\langle \tilde{t}_x \rangle$ is shown in the histogram in Figure 6. The average (mean) predicted values was $\overline{\langle \tilde{t}_x \rangle} = 0{\cdot}9946$ MPa (the overbar indicates mean value), which is slightly less than the true value of $\tilde{t}_x = 1$ MPa as shown in the figure. This indicates that regularization gives a biased solution. This is not surprising since in the regularization method, instead of solving the actual problem which has an unstable solution, a 'nearby' problem with a stable solution is solved which gives a 'nearby' result. The standard deviation in the predicted solution is $\sigma_{<\tilde{t}>} = 8{\cdot}53$ kPa, while the predicted standard deviation is $\sigma_{\tilde{t}} = 19{\cdot}66$ kPa. One true standard deviation $\sigma_{<\tilde{t}>}$ and one predicted standard deviation $\sigma_{\tilde{t}}$ are shown on either side of the average predicted traction $\overline{\langle \tilde{t}_x \rangle}$ in Figure 6 also. Because the solution is biased, the more conservative predicted standard deviation gives a safer result.

In the second example, a plate is loaded with both normal and shear stresses as shown in Figure 7. This example tests the algorithm with a problem that is not symmetric and which incorporates shear. The plate is assumed to be in a state of plane strain, and the plate is modelled with 70, eight-node isoparametric elements as shown. The plate has a length of $L_x = 7{\cdot}0$ m in the x direction and a length of $L_y = 8{\cdot}5$ m in the y direction and is fixed in both the x and y directions on the boundary $x = 0$. Again, the modulus of elasticity is $E = 30$ GPa and Poisson's ratio is $\nu = 0{\cdot}30$. The normal and shear traction distributions are

$$t_x(y) = 100\left[\frac{\sin h(1{\cdot}35 - 0{\cdot}2y)}{\sin h(1)} - (1{\cdot}35 - 0{\cdot}2y)\right]$$

$$t_y(y) = -\sin\left[\frac{2\pi(y - 1{\cdot}75)}{5}\right]$$

in MPa where $1{\cdot}75 \text{ m} < y < 6{\cdot}75$ m. As in the previous example, the problem is first solved directly, and then displacements at 'sensor' locations with superimposed random error are used as input to solve the inverse problem. In this case, the displacements at 28 'sensor' locations on another part of the boundary, which is known to be traction free, are taken as the measured data. This is a problem with unknown boundary conditions on one part of the boundary and overspecified boundary conditions on another part of the boundary. Only first-order regularization was used. The order of magnitude of the displacements in the x and y directions at the 'sensors' was $O(u_x) = O(u_y) = 0{\cdot}1$ mm. Uniform random error with $\varepsilon = 0{\cdot}001$ mm, or 1 per cent of $O(u_x)$ was added to the displacement data to stimulate measurement errors. The highest order of magnitude of α_1 that did not start to influence the solution significantly was $\alpha_1^1 = \alpha_1^2 = 10^{-5}$ $(\text{mm/MPa})^2$. The results for the normal and shear tractions along with error bars are plotted in Figures 8 and 9, respectively. It should be noted that the zero tractions on the boundary for $0 \text{ m} \leqslant y \leqslant 1{\cdot}75$ m and for $6{\cdot}75 \text{ m} \leqslant y \leqslant 8{\cdot}5$ m were assumed known. The error bars are taken as being plus or minus three standard deviations ($\pm 3\sigma_{\tilde{t}}$) which in the case of Gaussian distribution

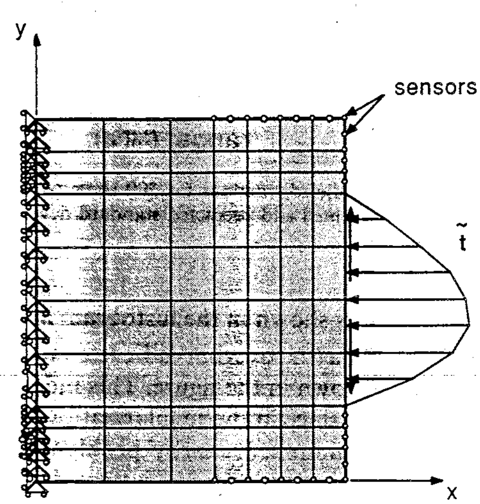

Figure 7. Geometry and loading condition for example 2

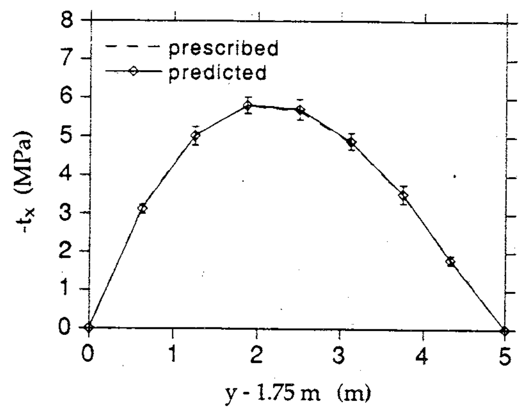

Figure 8. Predicted and actual normal tractions for example 2 using first-order regularization only with $\alpha_1^1 = \alpha_2^1 = 10^{-5}$ $(\text{mm/MPa})^2$

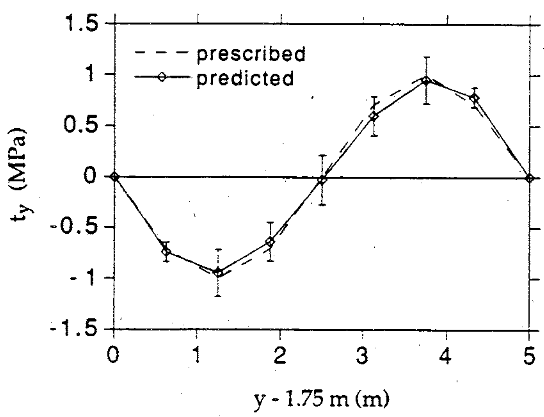

Figure 9. Predicted and actual shear tractions for example 2 using first-order regularization only with $\alpha_1^1 = \alpha_1^2 = 10^{-5}$ $(\text{mm/MPa})^2$

ensures a 99·7 per cent probability that the solution falls within the error bars. Since the error in the data is actually a uniform distribution, it is expected that the results are more conservative than for a Gaussian distribution, so three standard deviations should give a conservative error range. The actual solution in both cases falls within the error bars of the predicted solution.

8. CONCLUSION

A technique for estimating error in the solution of inverse elasticity problems based on a statistical analysis has been presented and compared with the spatial regularization method. This analysis provides additional insight into the significance of the regularization parameters and gives a method for estimating error in the solution.

Examples illustrating the effects of the order of regularization used, the magnitude of the regularization parameters, the error in the measured displacements and the location of the sensors on the accuracy of the solution have been investigated. Results from a Monte Carlo simulation were presented to compare the actual statistics of the solution with the predicted statistics. The predicted results were shown to give a conservative estimate for the standard deviation in the solution which is used to estimate error bars.

An example was also presented to demonstrate the applicability of the techniques to problems where the tractions and displacements are unknown on part of the boundary (which could represent a region of contact) while both tractions (in this case zero because of free surface) and approximate displacements (from measurements) are known on another part of the boundary.

While the statistical formulation provides a means for taking into account the modelization error, the modelization error has not been considered in the examples presented herein and is the subject of on-going research. To investigate this effect, it is necessary to examine problems with analytic solutions and to incorporate methods for estimating error in the finite element method.

ACKNOWLEDGEMENTS

The support of the Henry Luce Foundation, Inc. is gratefully acknowledged by Antoinette Maniatty.

REFERENCES

1. A. Tarantola, *Inverse Problem Theory: Methods for Data Fitting and Model Parameter Estimation*, Elsevier, New York, 1987.
2. D. S. Schnur and N. Zabaras, 'Finite element solution of two-dimensional inverse elasticity problems using spatial smoothing', *Int. j. numer. methods eng.*, **30**, 57–75 (1990).
3. G. M. L. Gladwell, *Inverse Problems in Vibrations*, Martinus Nijoff, Dordrecht, 1986.
4. H. R. Busby and D. M. Trujillo, 'Solution of an inverse dynamics problem using an eigenvalue reduction technique', *Comput. Struct.*, **25**, 109–117 (1987).
5. M. Bonnet, 'A numerical investigation for a source inverse problem in linear acoustics', *J. Acoustique*, **4**, 307–334 (1991).
6. A. Maniatty, N. Zabaras and K. Stelson, 'Finite element analysis of some inverse elasticity problems', *J. Eng. Mech. Div. ASCE*, **115**, 1302–1316 (1989).
7. N. Zabaras, V. Morellas and D. Schnur, 'A spatially regularized solution of inverse elasticity problems using the boundary element method', *Comm. appl. numer. methods*, **5**, 547–553 (1989)
8. N. Zabaras and D. Schnur, 'Solution of inverse elastic and elastoviscoplastic problems in two dimensions using the finite element method and spatial regularization', in *NUMETA '90, Numerical Methods in Engineering: Theory and Applications, Proc. 3rd Int. Conf.* University of Swansea, Swansea, Wales, January 7–11, 1990.
9. L. W. White, 'Estimation of elastic parameters in beams and certain plates: H_1 regularization', *J. Opt. Theory Appl.*, **60**, 305–329 (1989).
10. M. Ikehata, 'Inversion formulas for the linearized problem for an inverse boundary value problem in elastic prospection', *SIAM J. Appl. Math.*, **50**, 1635–1644 (1990).
11. T. Mura, 'A new NDT: evaluation of plastic strains in bulk from displacements on surfaces', *Mech. Res. Comm.*, **12**, 243–248 (1985).
12. Z. Gao and T. Mura, 'Nondestructive evaluation of interfacial damages in composite materials', *Int. J. Solids Struct.*, **25**, 901–916 (1989).
13. Z. Gao and T. Mura, 'On the inversion of residual stresses from surface displacements', *J. Appl. Mech. Div. ASME*, **56**, 508–513 (1989).
14. A. N. Tikhonov and V. Y. Arsenin, *Solution of Ill-Posed Problems*, V. H. Winston, Washington D.C., 1977.
15. J. V. Beck, B. Blackwell and C. R. St. Clair, *Inverse Heat Conduction: Ill-Posed Problems*, Wiley-Interscience, New York, 1985.
16. E. Artyukhin, 'Iterative algorithms for estimating temperature-dependent thermophysical characteristics', in *Inverse Problems in Engineering: Theory and Practice, Proc. 1st Int. Conf.*, Palm Coast, FL, ASME Press, New York, 1993.
17. P. Lamm, 'Inverse problems and Ill-posedness', in *Inverse Problems in Engineering: Theory and Practice, Proc. 1st Int. Conf.*, Palm Coast, FL, ASME Press, New York, 1993.